Three quantitative trait loci explain more than 60% of phenotypic variation for chill coma recovery time in *Drosophila ananassae*

4 Annabella Königer*, Saad Arif† and Sonja Grath*

5 * Division of Evolutionary Biology, Ludwig-Maximilians-Universität (LMU) München

6 82152 Planegg-Martinsried, Germany

7 † Department of Biological and Medical Sciences, Oxford Brookes University, Oxford,

8 OX3 0BP, United Kingdom

9

10

11

12

Keywords:

QTL mapping, RAD-Sequencing, cold tolerance, chill coma recovery time, *Drosophila ananassae*

Correspondence:

Sonja Grath

LMU Biocenter, Großhaderner Straße 2, 82152 Planegg-Martinsried, Germany

grath@bio.lmu.de

Tel.: +49 (0)89 / 2180-74110

Abstract

Ectothermic species such as insects are particularly vulnerable to climatic fluctuations. Nevertheless, many insects that evolved and diversified in the tropics have successfully colonized temperate regions all over the globe. To shed light on the genetic basis of cold tolerance in such species, we conducted a quantitative trait locus (QTL) mapping experiment for chill coma recovery time (CCRT) in *Drosophila ananassae*, a cosmopolitan species that has expanded its range from tropical to temperate regions.

We created a mapping population of recombinant inbred advanced intercross lines (RIAILs) from two founder strains with diverging CCRT phenotypes. The RIAILs were phenotyped for their CCRT and, together with the founder strains, genotyped for polymorphic markers with double-digest restriction site-associated DNA (ddRAD) sequencing. Using a hierarchical mapping approach that combined standard interval mapping and a multiple-QTL model, we mapped three QTL which altogether explained 64% of the phenotypic variance. For two of the identified QTL, we found evidence of epistasis. To narrow down the list of cold tolerance candidate genes, we cross-referenced the QTL intervals with genes that we previously identified as differentially expressed in response to cold in *D. ananassae,* and with thermotolerance candidate genes of *D. melanogaster*. Among the 58 differentially expressed genes that were contained within the QTL, *GF15058* showed a significant interaction of the CCRT phenotype and gene expression. Further, we identified the orthologs of four *D. melanogaster* thermotolerance candidate genes, *MtnA*, *klarsicht*, *CG5246* (*D.ana/GF17132*) and *CG10383* (*D.ana/GF14829*) as candidates for cold tolerance in *D. ananassae*.

Introduction

44 Temperature is one of the major factors that influence the geographical distribution and

45 abundance of ectothermic species. Physiological mechanisms to regulate body temperature

46 are usually limited in ectotherms and resilience towards temperature extremes often

47 determines the species fate upon climate change or range expansion. *Drosophila* spp. have

48 successfully mastered such thermal challenges as they colonized temperate regions all over

49 the globe and are now present on all of the earth's continents except Antarctica (Lachaise et

50 al., 1988). By far the most prominent example of the genus is *Drosophila melanogaster*,

51 which originated in sub-Saharan Africa, colonized temperate regions after the last

52 glaciation about 15,000 years ago and nowadays has a worldwide distribution (David and

53 Capy, 1988; Stephan and Li, 2007). Cold tolerance in this species has a highly polygenic

54 basis (von Heckel et al., 2016; MacMillan et al., 2016) and adaptation to local temperatures

55 required simultaneous selection at multiple loci (Morgan and Mackay, 2006; Svetec et al.,

56 2011).

57 Previously, we examined the cold tolerance of *Drosophila ananassae* (Königer and Grath,

58 2018), a tropical species which originated in South-East-Asia (Das et al., 2004). During the

59 past 18.000 years, *D. ananassae* expanded from its ancestral range to temperate regions and

60 has nowadays a quasi-cosmopolitan distribution (Das et al., 2004; Tobari, 1993) We

61 measured cold tolerance by means of a test for chill coma recovery time (CCRT), which is

62 defined as the time the flies need to stand on their legs after a cold-induced coma (David et

63 al., 1998). There was substantial variation in CCRT among fly strains that were derived

64 from a population of the ancestral species range in Bangkok, Thailand (Königer and Grath,

66 2018). Most strikingly, the difference in the phenotype within this single population was

67 large if compared to within-population variance in *D. melanogaster* (von Heckel et al.,

68 2016). However, in *D. ananassae*, only two genes, *GF15058* and *GF14647,* reacted to the

69 cold shock in a phenotype-specific, i.e., they showed a significant interaction of phenotype

70 and genotype.

71 Here, we report the results of a genome-wide scan for quantitative trait loci (QTL)

72 influencing CCRT in *D. ananassae.* To gain better insight into the genetic architecture of

73 cold tolerance in this species, we generated a mapping population of recombinant inbred

74 advanced intercross lines (RIAILs) from the most cold-tolerant strain and the most cold-

75 sensitive strain of the Bangkok population. By combining double-digest restriction site-

76 associated DNA sequencing (ddRAD) markers and a hierarchical mapping approach, we

77 identified three QTL of large effect which altogether explain 64% of the variance in the

78 phenotype. We further combined the present results with lists of genes that are differentially

79 expressed in response to the cold shock in *D. ananassae* (Königer and Grath, 2018) and *D.*

80 *melanogaster* (von Heckel et al., 2016).

81 Both species belong to the Melanogaster group and shared a common ancestor around 15-

82 20 million years ago (Drosophila 12 Genomes Consortium et al., 2007). *D. melanogaster*

83 expanded its range from Sub-Saharan Africa to temperate regions in Europe about 16,000

84 years ago (Stephan and Li, 2007). Our approach allowed us to narrow down the list of

85 potentially causal genes for cold tolerance and to uncover common evolutionary patterns

86 among species from completely independent phylogenetic lineages that have expanded

87 their thermal ranges and became successful human commensals.

Materials and Methods

Mapping population

All flies used in this study were raised on standard cornmeal molasses medium, at constant room temperature (22 ± 1°C) and at a 14:10 h light:dark cycle (details of the food recipe can be found in (Königer and Grath, 2018)). The two fly strains (Fast and Slow) that were used as founders for the mapping population were collected in 2002 in Bangkok, Thailand, and established as isofemale strains (Das et al., 2004). Recombinant Inbred Advanced Intercross Lines (RIAILs) were generated as follows (Figure 1): two initial crosses between the two parental strains were set up (Fast males x Slow females and Slow males x Fast females). Individuals from both F1 generations were mixed and allowed to mate freely with each other. Up to generation F4, intercrossing was continued in the form of mass breedings. In generation F4, 360 mating pairs were set up in separate vials to allow for one more generation of intercrossing and to initiate the inbred strains. From generation F5, full-sibling inbreeding was carried out by mating brother-sister pairs for five subsequent generations. Throughout all generations (P - F10), the parents were removed before the offspring hatched to avoid back-crosses. From generation F10 on, RIAILs were kept at low density in 50 ml vials.

Cold-sensitive (Slow) ♀   X   Cold-tolerant (Fast) ♂   Cold-tolerant (Fast) ♀   X   Cold-sensitive (Slow) ♂

F_1 X F_1

5 generations intercrosses/massbreeding

F_5 X   X   X

5 generations full-sib inbreeding

F_{10} Genotyping and phenotyping of 94 Recombinant inbred advanced intercross lines (RIAILs)
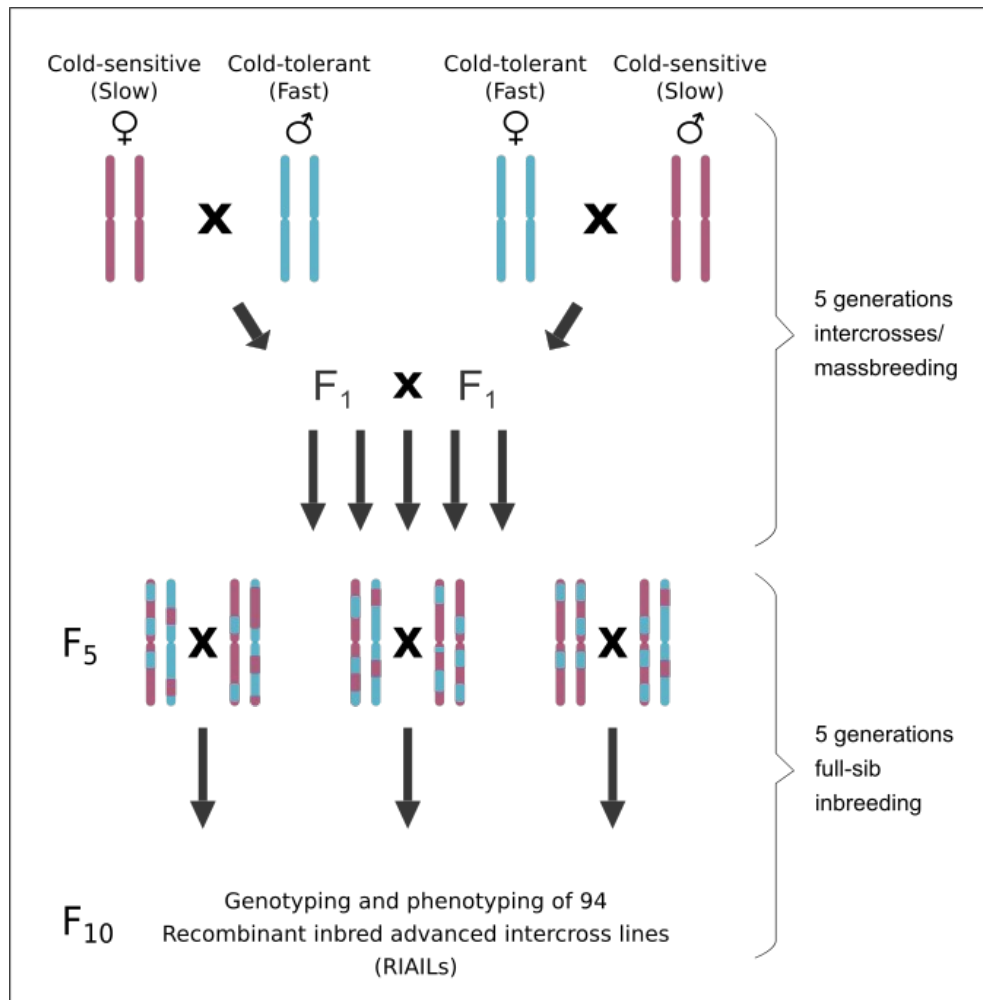
Figure 1. Crossing scheme for the generation of the RIAIL mapping population. Drawings of single chromosome pairs were used as representatives for the full genome. An initial, reciprocal cross between the cold-sensitive founder strain Slow (shown in red) and the cold-tolerant founder strain Fast (shown in blue) was set up to generate the heterozygous F1 generation. Intercrosses were continued in the form of massbreedings until generation F4, where single mating pairs were picked to allow for one more generation of intercrossing and to initiate inbreeding. From generation F5, full-sibling inbreeding was carried out for five subsequent generations. Throughout all generations (P - F10), the parents were removed before the offspring hatched to avoid back-crosses.

Test for chill coma recovery time (CCRT)

CCRT was measured for flies of 4 − 6 days of age as described previously (Königer and Grath, 2018). For the two founder strains Fast and Slow, CCRT was measured for males and females separately. For the RIAILs, only female flies were phenotyped. All female flies

133   were collected and phenotyped as virgins. In brief, collection and sex-separation were

134   carried out under light CO_2-anesthesia, whereby ten flies from the same sex and strain were

135   collected into a 50 ml vial containing 10 ml of cornmeal molasses medium. At the age of 4–

136   6 days, the flies were transferred without anesthesia into new vials without food. For the

137   cold shock, the vials were placed in an ice water bath (0 ± 0.5 °C) for exactly 3 h. Back at

138   room temperature (22 ± 1 °C), CCRT was monitored in 2 min intervals for the duration of

139   90 min. Flies that were still not standing after 90 min were assigned a recovery time of 92

140   min. Flies that died during the experiment (< 1 %) were excluded from the analysis. On

141   average, we tested 40 female individuals per RIAIL and 100 individuals per founder strain

142   and sex.

143

144   **DNA extraction and sequencing**

145   DNA was extracted from 94 RIAILs and the two parental strains with the DNeasy® Blood

146   & Tissue Kit (QIAGEN, Hilden, Germany). For each strain, 10 virgin female individuals

147   were pooled. DNA concentration and purity were assessed with a spectrophotometer

148   (NanoDrop® ND 1000, VWR International, Radnor, PA, USA). Library preparation and

149   double-digest restriction site-associated DNA sequencing (ddRAD-seq) was carried out by

150   an external sequencing service (ecogenics GmbH, Balgach, Switzerland) in the following

151   way: DNA was double-digested with EcoRI and MseI and ligated to respective adapters

152   comprising EcoRI and MseI restriction overhangs. Molecular identifier tags were added by

153   polymerase chain reaction. The individual sample libraries were pooled, and the resulting

154   library pools were size-selected for fragments between 500-600 bp with gel electrophoresis

155   and extraction of the respective size range. The resulting size selected library pools were

156   sequenced on a NextSeqTM 500 Sequencing System (Illumina, San Diego, CA), producing

157   single-ended reads of 75bp length. Demultiplexing and trimming from Illumina adapter

158   residuals was also carried out by the external service.

159

160   **Marker catalog construction and data curation**

161   The software pipeline Stacks (version 1.45) (Catchen et al., 2011) was used to analyze the

162   sequence data and to identify markers. First, to examine the quality of the sequence reads,

163   the *process_radtags* program was run in Stacks, applying a sliding window size of 50% of

164   the read length (*-w 0.5*) to filter out reads which drop below a 99% probability of being

165   correct (Phred score < 20) (*-s 20*). Second, the processed reads of each sample were

166   mapped to the *D. ananassae* reference genome (FlyBase release 1.05 (Attrill et al., 2016)

167   with NextGenMap (version 0.5.0) (Sedlazeck et al., 2013). Third, the mapped reads were

168   converted to bam format, sorted and indexed with samtools (version 0.1.18) (Li et al.,

169   2009). Fourth, the *ref_map.pl* wrapper program was run in Stacks, which executes the

170   Stacks core pipeline by running each of the Stacks components individually. In brief,

171   *pstacks* assembled RAD loci for each sample, *cstacks* created a catalog of RAD loci from

172   the two parental samples to create a set of all possible alleles expected in the mapping

173   population and *sstacks* matched all RIAIL samples against the catalog. The *genotypes*

174   program was executed last, applying automated corrections to the data (*-c*) to correct for

175   false-negative heterozygote alleles. Only those loci which were present in at least 80% of

176   the samples were exported (*-r 75*). Fifth, we applied additional corrections to the catalog by

177   running the *rxstacks* program with the following filtering settings: non-biological

178   haplotypes unlikely to occur in the population were pruned out (*--prune_haplo*), SNPs were

179   recalled once sequencing errors were removed using the bounded SNP model (*--*

180   *model_type_bounded*) with an error rate of 10% *(--bound_high 0.1*), and catalog loci with

181   an average log likelihood less than –200 were removed (*--lnl_lim -200.00*). Sixth, *cstacks*

182   and *sstacks* and *genotypes* (*-r 75*) were rerun to rebuild, match and export a new catalog

183   with the filtered SNP calls. *Load_radtags.pl* and *index_radtags.pl* were used to upload and

184   index the new catalog to a MySQL database. Seventh, a custom R script was used to

185   remove markers with extreme values of residual heterozygosity within RIAILs, using

186   cutoffs based on our inbreeding scheme (> 15% and < 35%) (Falconer and Mackay, 1996)

187   and to remove markers with an allele frequency drift < 10% from further analysis. Eighth,

188   the MySQL database was used to manually check the markers for errors. A total of 1,400

189   markers were included in the downstream analysis.

190

191   **Genetic map construction**

192   Genetic map construction was conducted with R/qtl (version 1.42) (Broman et al., 2003).

193   The function *countXO* was used to remove seven RIAILs with > 200 crossover events. One

194   more RIAIL was removed due to a low number of genotyped markers (< 700). The

195   downstream analysis included 1,400 markers and 86 RIAIL-samples (Supplementary file 1:

196   Table S3). Markers were partitioned into linkage groups based on a logarithm of the odds

197   (LOD) score threshold of 8 and a maximum recombination frequency (rf) of 0.35, assuming

198   a sequencing error rate of 1%. Map distances were calculated using the Haldane map

199   function. As a sanity check, the functions *plotRF* and *checkAlleles* were used to test for

200   potentially switched alleles and linkage groups were visually validated (based on rf and

201   LOD scores).

202

203   **Analysis of quantitative trait loci (QTL)**

204   QTL mapping was conducted with R/qtl (version 1.42) (Broman et al., 2003). Prior to

205   mapping, the genotype probabilities between marker positions were calculated with the

206   function *calc.genoprob* on a maximum grid size of 1 cM. To identify major QTL, standard

207   interval mapping was performed using the Expectation Maximization (EM) algorithm as

208   implemented with the *scanone* function. The results are expressed as a LOD score (Sen and

209   Churchill, 2001). Significance thresholds were calculated with 1,000 genome-wide

210   permutations. The initial single-QTL scan was extended with a more complex, two-

211   dimensional scan using Haley-Knott-Regression as implemented with the *scantwo* function.

212   Significance thresholds were again calculated with 1,000 genome-wide permutations.

213   To screen for additional QTL, estimate QTL effects and refine QTL positions, multiple-

214   QTL mapping (MQM) was performed (Arends et al., 2010). Here, missing genotypes were

215   simulated from the joint distribution using a Hidden Markov model with 1,000 simulation

216   replicates and an assumed error rate of 1% as implemented with the *sim.geno* function. The

217   MQM model was identified with a forward selection/backward elimination search

218   algorithm as implemented with the *stepwise* function, with the model choice criterion being

219   penalized LOD scores. The penalties were derived on the basis of the significance

220   permutations from the two-dimensional genome scan. To estimate the support interval for

221 each identified QTL, an approximate 95% Bayesian credible interval was calculated as

222 implemented by the *bayesint* function. Gene annotations for QTL intervals were

223 downloaded from FlyBase (Attrill et al., 2016) and screened for enriched GO terms and

224 KEGG pathways with DAVID (version 6.8) (Huang et al., 2009). Enrichment was

225 calculated against the background of all annotated genes (Attrill et al., 2016) using default

226 settings (EASE-score of 0.1 after multiple testing correction according to Benjamini-

227 Hochberg (Benjamini and Hochberg, 1995)). In addition, we cross-referenced the QTL

228 gene lists with lists of differentially expressed genes from a previously conducted

229 transcriptome analysis, where we compared gene expression among cold-tolerant and cold-

230 sensitive fly strains from the Bangkok population (including the two parental founder

231 strains used in this study) in response to the 3 h cold shock at 0°C (Königer and Grath,

232 2018). Moreover, the transcriptome analysis also comprises lists of differentially expressed

233 genes of cold-tolerant and cold-sensitive fly strains of *Drosophila melanogaster* in response

234 to a cold shock (von Heckel et al., 2016), allowing us to compare expression regulation of

235 orthologous genes within the QTL regions among these two *Drosophila* species.

236

237 **Data Availability**

238 The sequence data have been deposited in NCBI's Sequence Read Archive and are

239 accessible through series accession number PRJNA544044. Supplementary material is

240 deposited at figshare.

Results

Chill coma recovery time (CCRT) Phenotype

The average CCRT of the cold-tolerant founder strain (Fast) was 29.29 min for females and 30.13 min for males. CCRT of the cold-sensitive founder strain (Slow) was 63.70 min for females and 53.92 min for males (Figure 2, Supplementary file 1: Table S1). The difference in CCRT between the Fast strain and the Slow strain was significant for males (Welch's t-test, P-value $< 2.2 \times 10^{-16}$) and females (Welch's t-test, P-value $< 2.2 \times 10^{-16}$). The average CCRT of the RIAILs ranged from 27.60 min to 83.03 min (Figure 3, Supplementary file 1: Table S2).
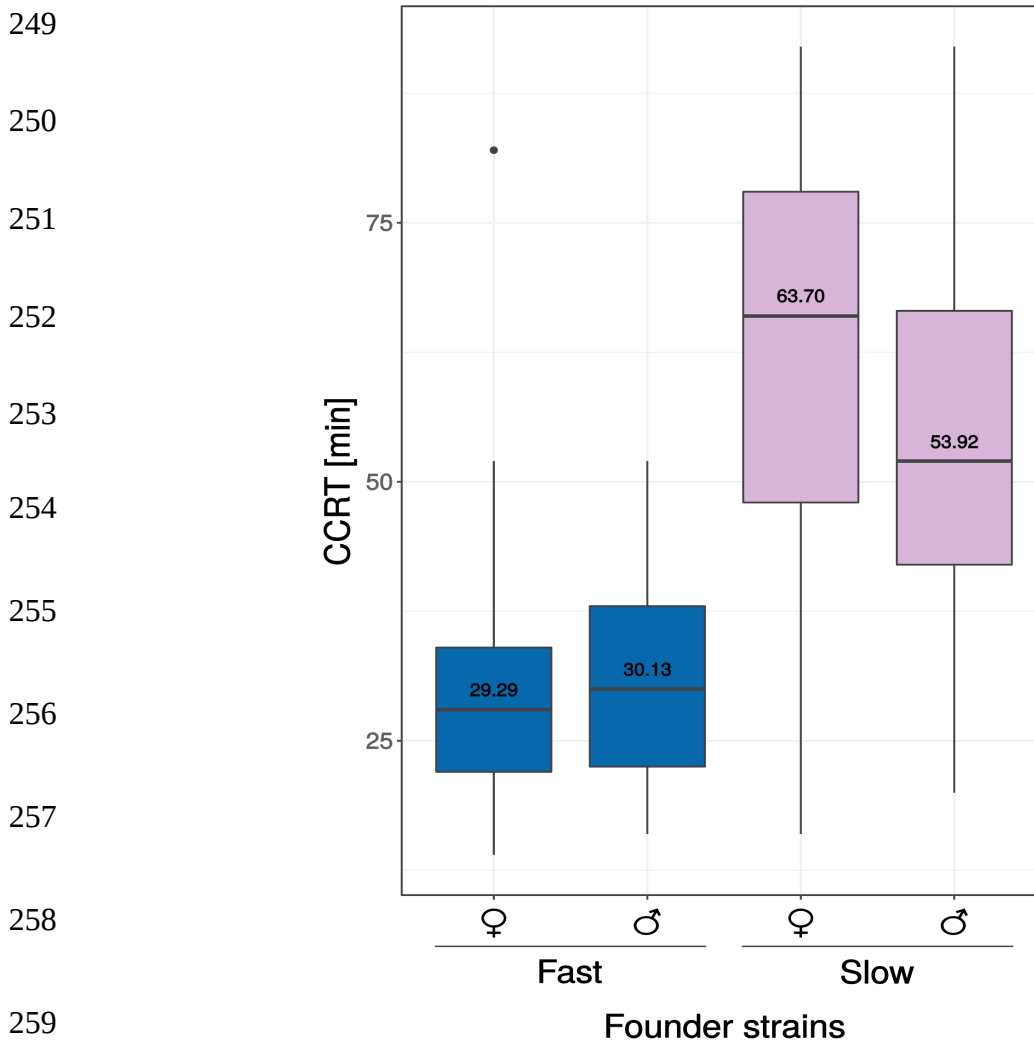
Figure 2. Chill coma recovery time (CCRT) of 4-6 day old flies of two strains of *D. ananassae* from Bangkok (Thailand) that were used as founder strains for the mapping population. In both sexes, the Fast strain recovered significantly faster than the Slow strain (Welch's t-test, *P*-value $< 2.2 \times 10^{-16}$).
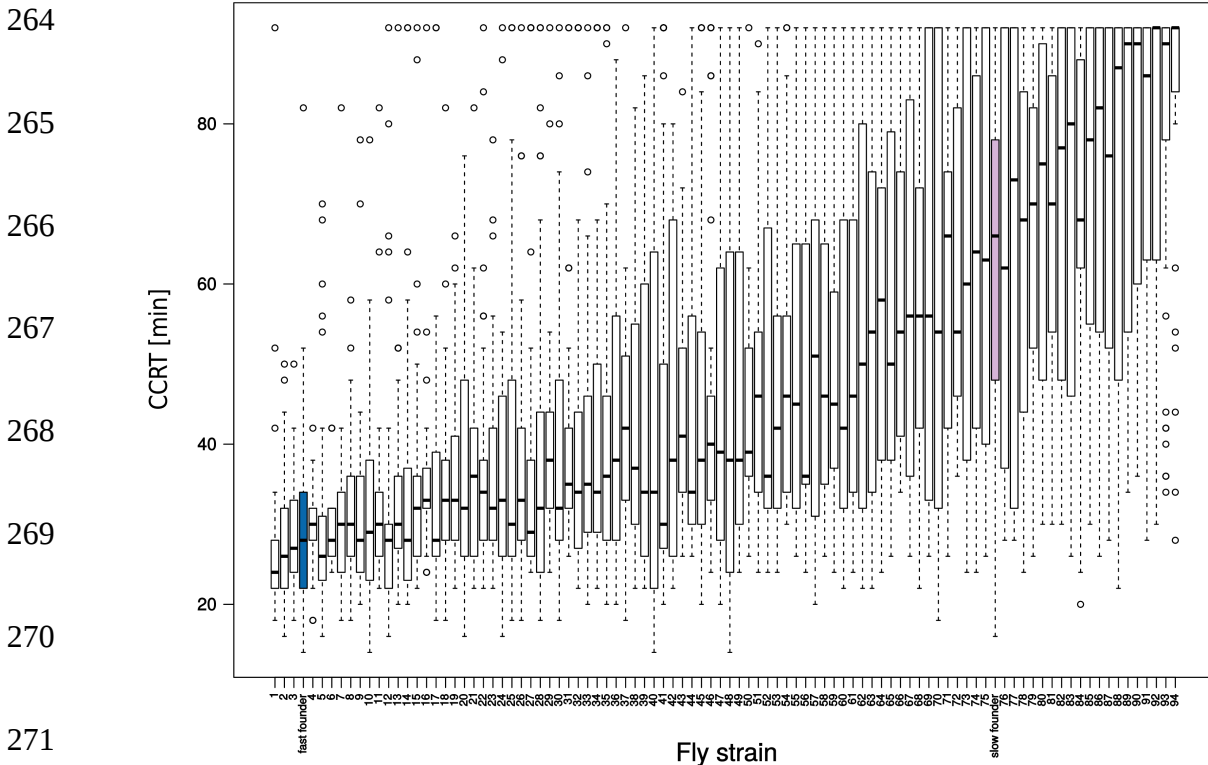
Figure 3. Chill coma recovery time (CCRT) of 4 - 6 day old virgin female flies of the 94 recombinant inbred advanced intercross lines (RIAILs) is displayed with white bars. CCRT of the two founder strains is displayed in blue (Fast founder) and pink (Slow founder) (see also Figure 2). The RIAILs were numbered in ascending order according to their average CCRT.

Sequencing and genetic map

In total, we obtained 331,867,133 sequence reads with an average of 3,281,450 reads per sample. 0.6% of the total reads (2,074,057) failed the Stacks *process_radtags* quality check and were excluded from the analysis. In each of the samples, > 94% of all reads mapped to the *D. ananassae* reference genome. The Stacks core pipeline matched 5,468 markers to the initial catalog. After additional corrections with the *rxstacks* program, 3,092 markers

13

283   remained. 1,692 more markers were excluded from this new catalog due to extreme values

284   of heterozygosity and allele frequency drift. Thus, after all filtering steps, a total of 1,400

285   markers and 86 RIAILs were used for genetic map construction. The markers were

286   partitioned into eight linkage groups (Supplementary file 1: Table S4). The total map length

287   was 962.0 cM, with an average marker spacing of 0.7 cM and a maximum marker spacing

288   of 55.5 cM (Figure 5). Across all samples, 91.6% of the genotypes were available of which

289   37.4% were homozygous for the cold-tolerant (Fast) allele (FF), 27.9% were heterozygous

290   (FS) and 34.7% were homozygous for the cold-sensitive (Slow) allele (SS).

291

292   **One- and two-dimensional genome scans**

293   Interval mapping in the context of a single-QTL model revealed two major areas with LOD

294   peaks which exceeded the permuted 5% significance level (LOD 3.53), one on scaffold

295   13337 (QTL1) and one on scaffold 13340 (QTL2) (Figure 4). The highest peak on scaffold

296   13337 was at 6.08 cM (LOD 5.80) and the highest peak on scaffold 13340 was at 80.05 cM
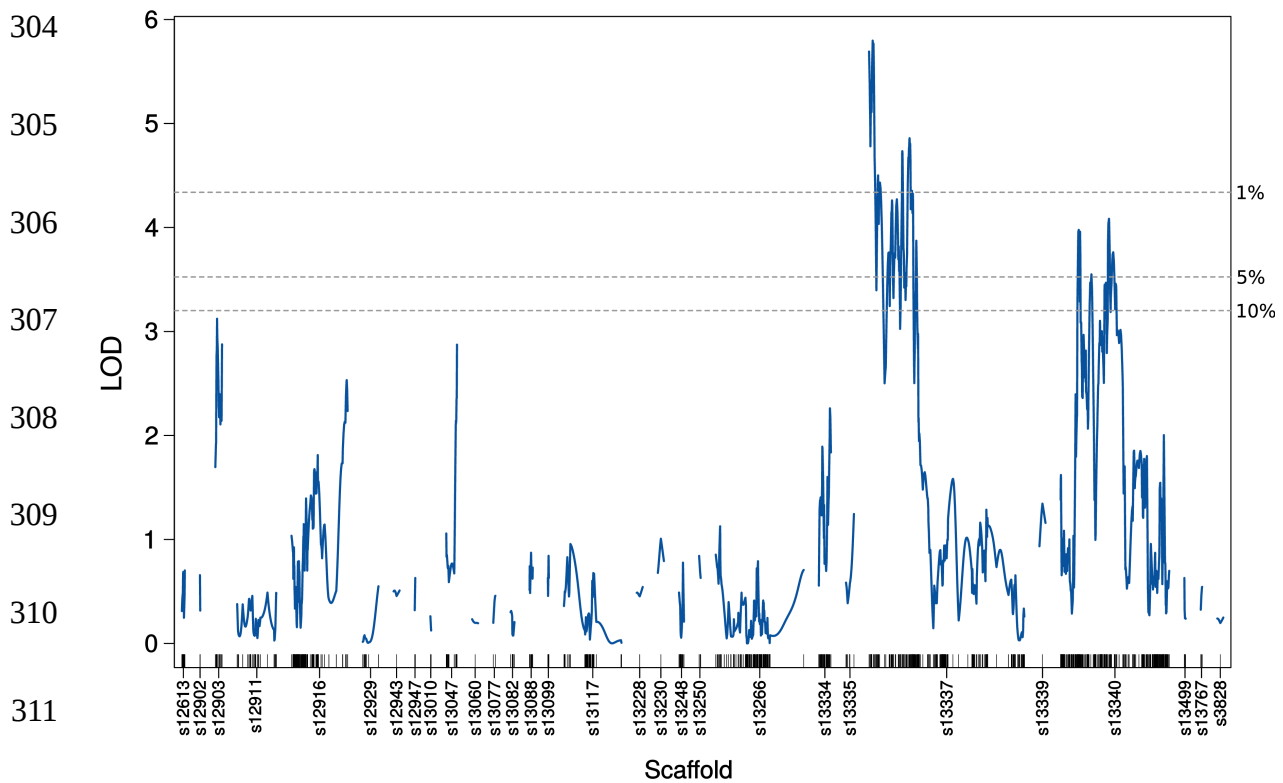
297   (LOD 4.08).

298

299

300

301

302

303

14

Figure 4. LOD-curves obtained with standard interval mapping reveal two significant QTL, QTL1 on scaffold 13337 and QTL2 on scaffold 14440. Significance thresholds (dotted lines) were calculated with 1,000 genome-wide permutations. The short vertical lines on the X-axis correspond to the marker positions.

The next step was to extend the initial, single-QTL scan with a two-dimensional scan, where we compared two possible models: the full (epistatic) model (H_{fl}) which allowed for the possibility of a second QTL and interactions among QTL was compared to the additive model (H_{a1}) which allowed for the possibility of a second QTL without interaction. Both the full and the additive model reached maximum LOD scores at the same positions, 7.08 cM on scaffold 13337 and 30.1 cM on scaffold 13340 (Table 1). In comparison to the single-QTL model, we found supporting evidence for the presence of a second QTL under the

15

325 additive model (lodd.av1 *P*-value = 0.006), but not under the full model (lod.fv1 *P*-value =

326 0.668). There is no evidence for interaction among the two loci (lod.int *P*-value = 1).

327

328 **Table 1.** Results of the two-dimensional genome scan

329

Two-QTL scan							
	pos1f[1]	pos2f[1]	lod.full[1]	*P*-value[1*]	lod.fv1[2]	*P*-value[2*]	
s13337:s13340	7.08	30.1	12.6	0	5.77	0.668	
	pos1a[3]	pos2a[3]	lod.add[3]	*P*-value[3*]	lod.av1[4]	*P*-value[4*]	lod.int[5]	*P*-value[5*]
s13337:s13340	7.08	30.1	11.4	0	4.54	0.006	1.24	1

332 **1)** QTL positions, LOD score and *P*-value for the full (epistatic) model versus the Null-model

333 **2)** LOD score and *P*-value for the full (epistatic) model versus the Single-QTL-model

334 **3)** QTL positions, LOD score and *P*-value for the additive model versus the Null-model

335 **4)** LOD score and *P*-value for the additive model versus the Single-QTL-model

336 **5)** LOD-score and *P*-value of (full model – additive model) = evidence for interaction

337 *) *P*-values represent the proportion of permutation replicates with LOD scores ≥ the observed

338

339 **Multilpe-QTL model**

340 In order to identify possible additional QTL of moderate effect, refine QTL positions,

341 separate linked loci and to estimate QTL effects, we applied a forward selection/backward

342 elimination algorithm with penalized LOD scores and identified a model with three main

343 terms and one interaction term. The overall fit of the model had a LOD score of 19.26 and

344 explained 64.34% of the phenotypic variance (Figure S2, Supplementary file 1: Table S5).

345 In comparison to the one- and two-dimensional genome-scans, there was an additional

346 locus on scaffold 12916 at position 16.7 cM (QTL3) which interacted with one of the

347 previously identified loci, on scaffold 13340 (QTL2) (Table 2, Figures 5, 6 and Figure S3).

348

Table 2. QTL confidence intervals and estimated effects

|	Scaffold	cytologic position [cM]	cytologic position [bp]	confidence interval [bp]	% variance	additive effect	dominance deviation	genes*
QTL1	13337	0.083871	0.083871 – 9.233870	83.871 – 226.785	26.59	9.2082	-2.1719	11
QTL2	13340	30.053110	27.51427 – 36.52024	5.542.036 – 6.544.039	30.44	1.7317	-5.2343	138
QTL3	12916	16.747634	7.103214 – 92.933043	1.514.827 - 2.696.582	19.89	-0.6307	-0.8054	110

QTL positions and effects on the phenotype as estimated with the multiple-QTL model. Confidence intervals were calculated as 95% Bayesian credible intervals.

* Numbers of protein-coding genes within QTL intervals. Numbers and identifiers for non-coding genes and RNAs are shown in Supplementary file 2.

QTL effects were estimated for additivity ((SS-FF)/2) and deviation from dominance ((FS-(FF+SS)/2), where F denotes the cold-tolerant Fast allele and S denotes the cold-sensitive Slow allele (Table 2, Supplementary file 1: Table S6). QTL3 on scaffold 12916 was a transgressive QTL as the cold-tolerant allele was associated with having a more cold-sensitive phenotype (longer CCRT), resulting in a negative effect size (Figure S1C). For QTL1, the estimated additive effect was positive while the estimated dominance effect was negative. RIAILs homozygous for the cold-tolerant allele had the most cold-tolerant phenotype, RIAILs homozygous for the cold-sensitive allele had the least cold-tolerant phenotype and heterozygote RIAILs had an intermediate phenotype (Figure S1A). The effect estimates for QTL2 went in the same direction as for QTL1. Here, however, the heterozygous phenotype was associated with the most cold-tolerant phenotype (Figure S1B). The more complex relationships of additive and dominance effects for the interaction of QTL3 and QTL2 can be understood best by plotting the interaction of the phenotype and the genotype at both marker positions (Figure 6).
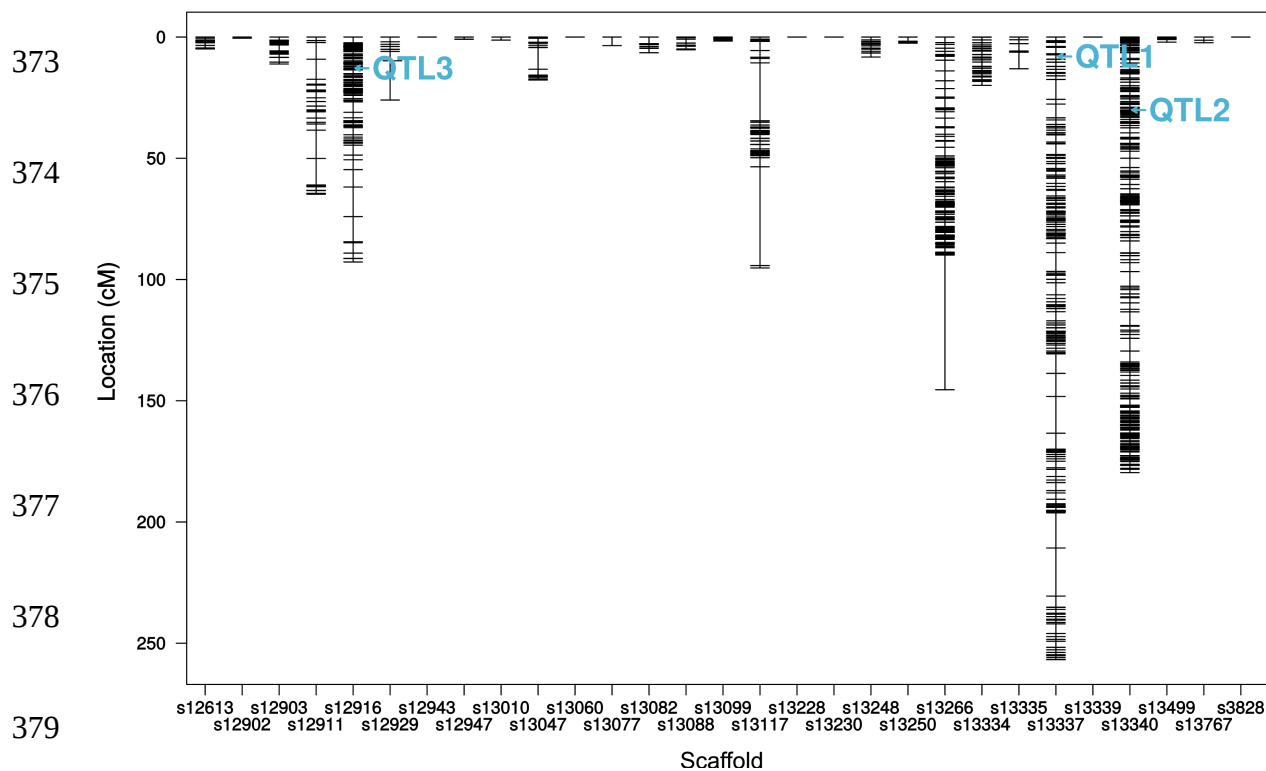
Figure 5. Genetic map with QTL positions as refined with the multiple-QTL model. X-axis = genomic scaffolds. Y-axis = genetic distances in centiMorgan (cM) for markers (short horizontal lines).
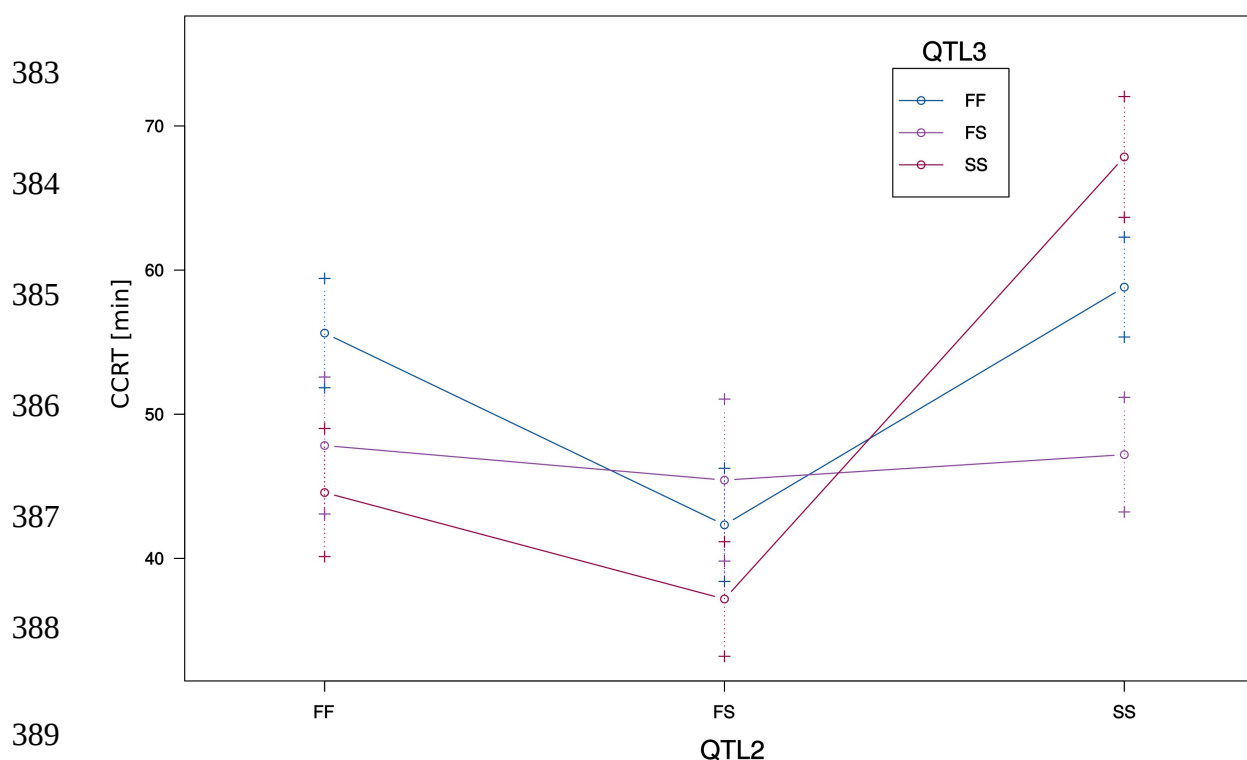
Figure 6. Interaction of QTL2 on scaffold 13340 and QTL3 on scaffold 12916. X-axis = genotypes for QTL2. The genotypes for QTL3 are represented by lines in different colors. Error bars are plotted at +/- 1 SE. F = cold-tolerant parental allele (fast CCR), S = cold-sensitive parental allele (slow CCR).

18

393 As revealed by the interaction plot (Figure 6), RIAILs homozygous for the cold-sensitive

394 (S) allele at both QTL also had the most cold-sensitive phenotype. The most cold-tolerant

395 phenotype, was reached by those RIAILs which were homozygous for the cold-tolerant

396 allele at QTL2 but homozygous for the cold-sensitive allele at (the transgressive) QTL3

397 Interestingly, cold tolerance of RIAILs which were heterozygous at QTL3 seemed to be

398 independent from their genotype at QTL2.

399 The results of a drop-one-term at a time ANOVA indicated strong evidence for all three loci

400 and the interaction of QTL2 and QTL3: for each QTL, the model with the QTL of interest

401 at that particular position was compared to the model with the QTL of interest omitted,

402 while all other QTL positions were fixed at their maximum likelihood estimates (Table 3,

403 Figure S3).

404

405 **Table 3** Summary table for the drop one term ANOVA

406

QTL	cytologic position	df	Type III SS	LOD	%Var	F value	P (Chi2)	P (F)
1	s13337-0.1	2	4903	10.404	26.59	27.962	0	8.45E-10
2	s13340-30.1	6	5613	11.526	30.44	10.671	0	1.52E-08
3	s12916-16.7	6	3667	8.277	19.89	6.972	0	6.47E-06
2:3	s13340-30.1:s12916-16.7	4	2790	6.606	15.13	7.957	0	2.11E-05

408 S13337-0.1 = QTL on scaffold 13337 at position 0.1 cM, df = degrees of freedom, SS = sums of squares, MS
409 = mean squares, LOD = relative to the null model, %Var = proportion of variance in the phenotype explained
410 by all terms in the model, P (Chi2) = P-value based on LOD score following a χ 2-distribution, P(F) = P-
411 value based on the F-statistic. Profile LOD scores are shown in Figure S3.

412

413

414

415   **Candidate gene meta analysis**

416   All three QTL together contained 259 protein-coding genes (Table 4, Supplementary file 2:

417   Tables S1, S2, S5). Among them were 58 genes that we had identified previously as

418   differentially expressed in response to the cold shock (Königer and Grath, 2018, Table 4).

419

420   **Table 4.** Cold tolerance candidate genes within QTL regions

DE genes		Cold tolerance candidate genes
QTL1	3	*GF24896* (D.mel/*klarsicht*, MacMillan et al., 2016)
QTL2	26	*MtnA (D.mel/MtnA, Catalán et al., 2016), GF17132 (D.mel/CG5246, von Heckel et al., 2018)*
QTL3	29	*GF14829* (D.mel/*CG10383*, Norry et al. 2008), *GF15058* (Königer and Grath, 2018)

423   DE genes = differentially expressed genes in response to the cold shock as identified by Königer and
424   Grath, 2018. DE genes are listed in Supplementary file 2: Tables S1, S2 and S5.
425   Cold tolerance candidate genes = genes previously identified as candidates for cold tolerance in *D.*
426   *melanogaster.*
427

428   QTL1 spanned 140 kb and contained eleven protein coding genes (Supplementary file 2:

429   Table S1). There was no enrichment of KEGG pathways or GO terms. However, three of

430   the eleven genes were previously identified to be differentially expressed in response to a

431   cold shock (Supplementary file 2: Table S1, (Königer and Grath, 2018). Two of them,

432   *GF24884* (ortholog of *p130CAS*) and *GF24880* (ortholog of *Phosphoinositide-dependent*

433   *kinase 1*) were upregulated in both phenotypes after the cold shock and one of them,

434   *GF24896* (ortholog of *klarsicht*) was exclusively upregulated in the cold-tolerant phenotype

435   only. Klarsicht was previously reported as upregulated in cold-acclimated flies of *D.*

436   *melanogaster* (MacMillan et al., 2016).

20

437   QTL2 spanned 1.0 Mb and contained 138 protein coding genes which were enriched in one

438   molecular function, "serine-type endopeptidase activity" (GO:0004252) and one biological

439   process, "intracellular cholesterol transport" (GO:0032367) (Supplementary file 2: Table

440   S3). Out of the 138 genes, 26 were previously identified as differentially expressed in

441   response to a cold shock. Among them, nine genes were upregulated and five genes were

442   downregulated in both phenotypes (see Supplementary file 2: Table S2, and (Königer and

443   Grath, 2018)). In the cold-tolerant phenotype, one gene, *GF17809* (ortholog of *Archease*)

444   was exclusively upregulated and one gene, *GF17856* (ortholog of *Niemann-Pick type C-2c*)

445   was exclusively downregulated. In the cold-sensitive phenotype, one gene, *GF17176*

446   (ortholog of *aluminum tubes*) was exclusively upregulated and nine genes were exclusively

447   downregulated (see Supplementary file 2: Table S2, and (Königer and Grath, 2018).

448   Nine genes drove the enrichment in the GO category "serine-type endopeptidase activity"

449   (see Supplementary file 2: Table S3). All of them were located in the downstream region of

450   QTL2 at 6,515,565 - 6,527,729 bp and adjacent to one another (Figure 7). Seven of these

451   genes were also differentially expressed in response to cold shock. Among them was

452   *GF17132,* which was upregulated in both phenotypes and its ortholog in *D. melanogaster*

453   showed a significant interaction of phenotype and cold shock (Supplementary file 2: Table

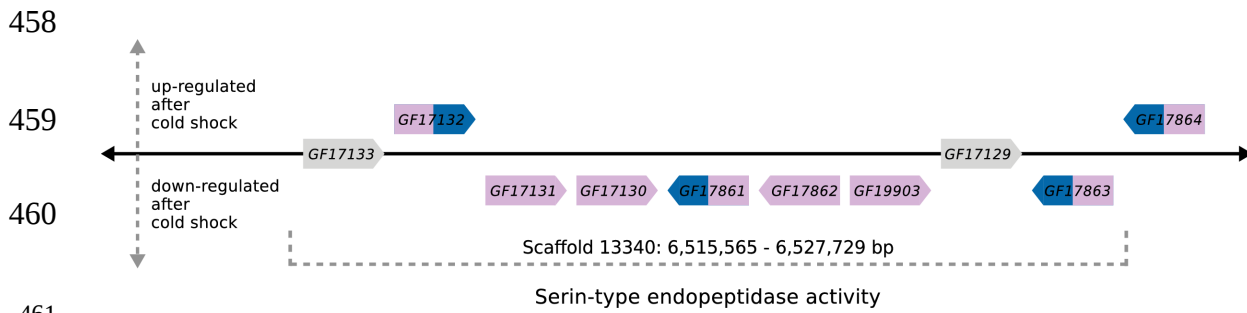454   S2, von Heckel et al., 2016).

455

456

457

Figure 7. Schematic illustration of a genomic region within QTL2 that contains nine genes of the enriched GO category "serine-type endopeptidase activity" (see also Supplementary file 2: Table S2 and S3). Genes were differentially expressed in response to the cold shock in either the cold-sensitive (slow) phenotype alone (genes shown in pink color) or in both phenotypes, cold-sensitive and cold-tolerant (fast) (genes shown in blue and pink color). Genes that were not differentially expressed are shown in grey. Gene lengths and distances between genes are not drawn to scale.

QTL2 also contained the gene *Metallothionein A* (*MtnA*) which caught our attention because it is involved in metal ion homeostasis and in its *D. melanogaster* ortholog, an InDel polymorphism is associated with local adaptation to oxidative stress upon migration out of Sub-Saharan Africa into Europe (Catalán et al., 2016). *MtnA* was downregulated in response to cold in *D. melanogaster* (von Heckel et al., 2016) but not in *D. ananassae* (Königer and Grath, 2018).

QTL3 spanned 1.2 Mb and contained 110 protein coding genes which were enriched in three molecular functions: "sequence-specific DNA binding" (GO:0043565), "ATPase activity" (GO:0016887) and "phosphotransferase activity, alcohol group as acceptor" (GO:0016773) and one KEGG pathway: "Hippo signaling pathway – fly" (dan04391) (Supplementary file 2: Table S6). Out of the 110 genes, 29 were previously identified as differentially expressed in response to a cold shock (Table 4). Among them, 12 genes were upregulated and seven genes were downregulated in both phenotypic groups, cold-tolerant

482   and cold-sensitive (see Supplementary file 2: Table S5, (Königer and Grath, 2018)). In the

483   cold-tolerant phenotype, two genes, *GF15043* (ortholog of *CG31974*) and *GF14846*

484   (ortholog of *bicoid stability factor*) were exclusively upregulated and two genes, *GF15020*

485   (ortholog of *ABC transporter expressed in trachea*) and *GF14865* (ortholog of *CG11454*)

486   were exclusively downregulated. In the cold-sensitive phenotype, five genes were

487   exclusively downregulated but there were no exclusively upregulated genes. One of the five

488   downregulated genes was *GF15058* (ortholog of *CG10178*), which was one out of two

489   genes with a significant interaction of phenotype and cold shock. The function of *GF15058*

490   is unknown but it is predicted to have UDP-glycosyl-transferase-activity (Marchler-Bauer

491   et al., 2015).

492

493

494

495

496

497

498

499

500

501

Discussion

502   **Discussion**

503   We used a panel of 86 recombinant inbred advanced intercross lines (RIAILs) and 1,400

504   ddRAD markers to map QTL that underlie natural variation in cold tolerance among two fly

505   strains of *D. ananassae* from a population in Bangkok, Thailand. The recovery time

506   segregated significantly between the two founder strains. CCRT in the cold-sensitive strain

507   was about twice as high as in the cold-tolerant strain. This observation was of particular

508   interest to us because in *D. melanogaster*, previous studies found such differences in the

509   CCRT phenotype only among different populations that inhabit different thermal habitats

510   (David et al., 1998; von Heckel et al., 2016).

511   The CCRT phenotypes of the mapping population were distributed on a continuum (Figure

512   3), which was a first important indicator that we were looking at more than one dominant

513   causal allele. Furthermore, three RIAILs recovered faster than the Fast parental strain and

514   19 of the RIAILs recovered slower than the Slow parental strain, indicating that there was

515   interaction among the parental alleles or loci in the recombinant genotypes of the mapping

516   population.

517   The three identified QTL for CCRT explain as much as 64% of the variance in the

518   phenotype. This proportion is equal to a previous mapping experiment for CCRT in *D.*

519   *melanogaster*, in which three QTL explained 64% of the variance for CCRT in an

520   intercontinental set of recombinant inbred lines (Norry et al., 2008). The founder strains for

521   this mapping population were sampled from Denmark and Australia and thus from two

522   geographically different thermal environments. Another study (Morgan and Mackay, 2006)

24

523 also identified three QTL for CCRT in *D. melanogaster* in a set of recombinant inbred lines

524 derived from two laboratory strains that differed significantly for the phenotype. In this

525 mapping population, the three loci explained 25% of the phenotypic variance for CCRT.

526 While two of the reported QTL for CCRT in *D. melanogaster* co-localized across these two

527 studies, none of the reported candidate genes co-localize with the QTL intervals in *D.*

528 *ananassae* (this study).

529 It needs to be noted that, in general, QTL confidence intervals should be considered as

530 support regions rather than absolute boundaries (Broman and Sen, 2009). Further, the

531 causal genetic variants may be located anywhere within these intervals.

532 Compared to sequencing of pooled samples (Pool-sequencing), RAD-based approaches

533 come at the cost of marker density, especially in crossing designs with low genetic

534 differentiation between the founder strains and low levels of linkage disequilibrium

535 (Futschik and Schlötterer, 2010). Thus, to increase the mapping resolution and to expand

536 the genetic map, we generated a mapping population in which five generations of

537 intercrosses allowed for a sufficient number of crossover events (Pollard, 2012).

538 Subsequently, we used stringent cutoffs for potential sequencing errors and distorted loci.

539 This step certainly increased the robustness of the identified loci, but came at the cost of

540 chromosomal coverage, as many smaller genomic scaffolds were excluded from the

541 analysis at this step. It is therefore possible that our results do not cover all potential QTL.

542 However, the reduction of genome complexity that results from RAD-sequencing has two

543 major benefits. First, it is more cost-effective than whole-genome sequencing of individual

544 samples, allowing for a larger number of samples to be analyzed and consequently for

25

545 greater statistical power to detect QTL. Second, it is more accurate than whole-genome

546 Pool-sequencing (Catchen et al., 2017; Cutler and Jensen, 2010).

547 Combining the identified intervals with two previous transcriptome analyses in *D.*

548 *ananassae* (Königer and Grath, 2018) and *D. melanogaster* (von Heckel et al., 2016) and

549 additional cold tolerance studies in *D. melanogaster* (MacMillan et al., 2016; Norry et al.,

550 2008; Ramnarine et al., 2019) allowed us to narrow down the list of potentially causal

551 genes in *D. ananassae* and to identify common candidate genes in both species. From the

552 combined data, we identified three types of candidates:

553 **I)** The expression profile of *GF15058* (*D.mel/CG10178*) in QTL3 is directly associated

554 with a difference in the CCRT phenotype in *D. ananassae*. *GF15058* was one out of two

555 genes that responded to the cold shock in a phenotype-specific way (Königer and Grath,

556 2018). Its function was inferred from electronic annotation to be uridine diphosphate (UDP)

557 glycosyltransferase activity. UDP-glycosyltransferases (UGTs) are membrane-bound

558 enzymes that are located in the endoplasmatic reticulum and catalyze the addition of a

559 glycosyl group from a uridine triphosphate (UTP) sugar to a small hydrophobic molecule.

560 Therefore, UGTs play an essential role in maintaining homeostatic function and

561 detoxification and are known as major members of phase II drug metabolizing enzymes

562 (Bock, 2015). The cold shock led to a downregulation of *GF15058* in the Slow strains but

563 not in the Fast strains. However, the Fast genotype at QTL3 is transgressive, i.e., it

564 increases CCRT. Thus, if *GF15058* was indeed one of the causal factors, our results suggest

565 that keeping transcript abundance at a constant level after the cold shock is so costly for the

566 organism that it slows down recovery.

567 **II)** The expression profile of *GF17132* (*D.mel*/*CG5246*) in QTL2 is directly associated with

568 a difference in the CCRT phenotype in *D. melanogaster*, where it showed a significant

569 interaction of phenotype and cold shock (von Heckel et al., 2016). It was also differentially

570 expressed in response to the cold shock in *D. ananassae* (Königer and Grath, 2018).

571 Moreover, *GF17132* belongs to a cluster of genes that code for serine peptidases in QTL2

572 (Figure 7). Serine peptidases are involved in proteolysis, i.e., they catalyze the hydrolysis of

573 peptide bonds (Attrill et al., 2016; Ross et al., 2003). This process plays a central role in the

574 immune response of insects (De Gregorio et al., 2001) and serine proteases were suggested

575 previously to be involved in the cold stress response as well (Vermeulen et al., 2013).

576 **III)** We identified three more genes that have been associated with thermotolerance in

577 experiments other than the transcriptome analyses: *MtnA* (*D.mel*/*MtnA*), *GF24896*

578 (*D.mel/klarsicht)* and *GF14829* (*D.mel/CG10383*).

579 The gene *MtnA* in QTL2 codes for metallothionein A which promotes resistance to

580 oxidative stress. It binds heavy metals and neutralizes reactive oxygen and nitrogen species

581 (Ruttkay-Nedecky et al., 2013). Exposure to cold leads to an increased abundance of free

582 radicals, thereby inducing oxidative stress (Williams et al., 2014). In *D. melanogaster*, a 49

583 bp deletion in the 3'UTR of *MtnA* is associated with its transcriptional upregulation and

584 with increased tolerance to oxidative stress (Catalán et al., 2016). The frequency of this

585 polymorphism in natural populations follows latitudinal clines, suggesting that upregulation

586 of *MtnA* is favored in temperate environments (Ramnarine et al., 2019). However, a direct

587 link between cold stress and oxidative stress is yet to be established in drosophilids

588 (Plantamp et al., 2016). *MtnA* was downregulated after the cold shock in both phenotypes

589　of *D. melanogaster* (von Heckel et al., 2016) and not differentially expressed in *D.*

590　*ananassae*. Moreover, a previous sequence analysis of *MtnA* in *D. ananassae* reported the

591　3'UTR deletion polymorphism as absent in 110 strains that were sampled in tropical and

592　temperate regions around the world (Stephan et al., 1994).

593　The gene *GF24896* (*D.mel/klarsicht*) in QTL1 is expressed in a wide range of tissues,

594　where it interacts with microtubules and promotes evenly spaced positioning of nuclei.

595　Knock-out of *klarsicht* in muscle cells impairs locomotion and flight (Elhanany-Tamir et

596　al., 2012) – functions that are also disabled during chill coma. The gene was reported

597　previously to be upregulated with cold-acclimation in *D. melanogaster (MacMillan et al.,*

598　*2016)*. In *D. ananassae*, *GF24896* is upregulated after the cold shock in Fast strains but not

599　in Slow strains (Königer and Grath, 2018), suggesting a potential contribution of this gene

600　to faster recovery from cold exposure.

601　Lastly, the gene *GF14829* (*D.mel*/*CG10383*) in QTL3 is involved in the regulation of

602　glycosylphosphatidylinositol metabolism. After the cold shock, it is upregulated in Fast and

603　Slow strains of *D. ananassae* and in Slow strains of *D. melanogaster*. Interestingly, over-

604　expression of *CG10383* increases lifespan in *D. melanogaster (Paik et al., 2012)*. It was

605　also the only gene within all three QTL for CCRT in *D. ananassae* that mapped to a heat-

606　tolerance QTL in *D. melanogaster* (Norry et al., 2008). In the face of the transgressive

607　nature of QTL3, potential allelic effects resulting in trade-offs between CCRT, heat-

608　resistance and lifespan should be investigated in both species.

609　In conclusion, we identified three large-effect QTL for recovery from cold exposure in *D.*

610　*ananassae*. Combining the present results with previous results obtained from *D.*

28

611   *melanogaster* allowed us to shed light on commonalities and differences in the genetic basis

612   of cold tolerance between these two species from different phylognetic lineages that have

613   independently expanded their thermal ranges an became successful human commensals.

614   The combined data point at the five above mentioned genes as candidates for recovery from

615   cold exposure. These genes serve as the groundwork for more detailed analyses such as

616   loss-of-function experiments to establish a link between genotype and phenotype in both

617   species.

618

619   **References**

Arends, D., Prins, P., Jansen, R.C., and Broman, K.W. (2010). R/qtl: high-throughput multiple QTL mapping. Bioinforma. Oxf. Engl. *26*, 2990–2992.

Attrill, H., Falls, K., Goodman, J.L., Millburn, G.H., Antonazzo, G., Rey, A.J., and Marygold, S.J. (2016). FlyBase: establishing a Gene Group resource for *Drosophila melanogaster*. Nucleic Acids Res. *44*, D786–D792.

Benjamini, Y., and Hochberg, Y. (1995). Controlling the False Discovery Rate: A Practical and Powerful Approach to Multiple Testing. J. R. Stat. Soc. Ser. B Methodol. *57*, 289–300.

Bock, W. (2015). The UDP-glycosyltransferase (UGT) superfamily expressed in humans, insects and plants: Animal-plant arms-race and co-evolution. Biochem. Pharmacol. *99*.

Broman, K., and Sen, S. (2009). A Guide to QTL Mapping with R/qtl (New York: Springer-Verlag).

Broman, K.W., Wu, H., Sen, S., and Churchill, G.A. (2003). R/qtl: QTL mapping in experimental crosses. Bioinforma. Oxf. Engl. *19*, 889–890.

Catalán, A., Glaser-Schmitt, A., Argyridou, E., Duchen, P., and Parsch, J. (2016). An Indel Polymorphism in the MtnA 3' Untranslated Region Is Associated with Gene Expression Variation and Local Adaptation in *Drosophila melanogaster*. PLoS Genet. *12*.

Catchen, J.M., Amores, A., Hohenlohe, P., Cresko, W., and Postlethwait, J.H. (2011). Stacks: Building and Genotyping Loci De Novo From Short-Read Sequences. G3 GenesGenomesGenetics *1*, 171–182.

Catchen, J.M., Hohenlohe, P.A., Bernatchez, L., Funk, W.C., Andrews, K.R., and Allendorf, F.W. (2017). Unbroken: RADseq remains a powerful tool for understanding the genetics of adaptation in natural populations. Mol. Ecol. Resour. *17*, 362–365.

Cutler, D.J., and Jensen, J.D. (2010). To Pool, or Not to Pool? Genetics *186*, 41–43.

Das, A., Mohanty, S., and Stephan, W. (2004). Inferring the Population Structure and Demography of *Drosophila ananassae* From Multilocus Data. Genetics *168*, 1975–1985.

David, J.R., and Capy, P. (1988). Genetic variation of *Drosophila melanogaster* natural populations. Trends Genet. TIG *4*, 106–111.

David, J., Gibert, P., Pla, E., Petavy, G., Karan, D., and Moreteau, B. (1998). Cold stress tolerance in *Drosophila*: Analysis of chill coma recovery in *D. Melanogaster*. J. Therm. Biol. *23*, 291–299.

De Gregorio, E., Spellman, P.T., Rubin, G.M., and Lemaitre, B. (2001). Genome-wide analysis of the *Drosophila* immune response by using oligonucleotide microarrays. Proc. Natl. Acad. Sci. U. S. A. *98*, 12590–12595.

Drosophila 12 Genomes Consortium, Clark, A.G., Eisen, M.B., Smith, D.R., Bergman, C.M., Oliver, B., Markow, T.A., Kaufman, T.C., Kellis, M., Gelbart, W., et al. (2007). Evolution of genes and genomes on the *Drosophila* phylogeny. Nature *450*, 203.

Falconer, and Mackay (1996). Introduction to Quantitative Genetics (Edinburgh/London: Oliver & Boyd).

von Heckel, K., Stephan, W., and Hutter, S. (2016). Canalization of gene expression is a major signature of regulatory cold adaptation in temperate *Drosophila melanogaster*. BMC Genomics *17*.

Huang, D.W., Sherman, B.T., and Lempicki, R.A. (2009). Systematic and integrative analysis of large gene lists using DAVID bioinformatics resources. Nat. Protoc. *4*, 44–57.

Königer, and Grath (2018). Transcriptome analysis reveals candidate genes for cold tolerance in *Drosophila ananassae*. Genes (Basel) 12;9(12).

Lachaise, D., Cariou, M.-L., David, J.R., Lemeunier, F., Tsacas, L., and Ashburner, M. (1988). Historical Biogeography of the *Drosophila melanogaster* Species Subgroup. In Evolutionary Biology, M.K. Hecht, B. Wallace, and G.T. Prance, eds. (Boston, MA: Springer US), pp. 159–225.

Li, H., Handsaker, B., Wysoker, A., Fennell, T., Ruan, J., Homer, N., Marth, G., Abecasis, G., Durbin, R., and 1000 Genome Project Data Processing Subgroup (2009). The Sequence Alignment/Map format and SAMtools. Bioinforma. Oxf. Engl. *25*, 2078–2079.

MacMillan, H.A., Knee, J.M., Dennis, A.B., Udaka, H., Marshall, K.E., Merritt, T.J.S., and Sinclair, B.J. (2016). Cold acclimation wholly reorganizes the *Drosophila melanogaster* transcriptome and metabolome. Sci. Rep. *6*, 28999.

Marchler-Bauer, A., Derbyshire, M.K., Gonzales, N.R., Lu, S., Chitsaz, F., Geer, L.Y., Geer, R.C., He, J., Gwadz, M., Hurwitz, D.I., et al. (2015). CDD: NCBI's conserved domain database. Nucleic Acids Res. *43*, D222-226.

Morgan, T.J., and Mackay, T.F.C. (2006). Quantitative trait loci for thermotolerance phenotypes in *Drosophila melanogaster*. Heredity *96*, 232–242.

Norry, F.M., Scannapieco, A.C., Sambucetti, P., Bertoli, C.I., and Loeschcke, V. (2008). QTL for the thermotolerance effect of heat hardening, knockdown resistance to heat and chill-coma recovery in an intercontinental set of recombinant inbred lines of *Drosophila melanogaster*. Mol. Ecol. *17*, 4570–4581.

Paik, D., Jang, Y.G., Lee, Y.E., Lee, Y.N., Yamamoto, R., Gee, H.Y., Yoo, S., Bae, E., Min, K.-J., Tatar, M., et al. (2012). Misexpression screen delineates novel genes controlling *Drosophila* lifespan. Mech. Ageing Dev. *133*, 234–245.

Plantamp, C., Salort, K., Gibert, P., Dumet, A., Mialdea, G., Mondy, N., and Voituron, Y. (2016). All or nothing: Survival, reproduction and oxidative balance in Spotted Wing *Drosophila* (*Drosophila suzukii*) in response to cold. J. Insect Physiol. *89*, 28–36.

Ramnarine, T.J.S., Glaser-Schmitt, A., Catalán, A., and Parsch, J. (2019). Population Genetic and Functional Analysis of a cis-Regulatory Polymorphism in the *Drosophila melanogaster* Metallothionein A gene. Genes *10*.

Ross, J., Jiang, H., Kanost, M.R., and Wang, Y. (2003). Serine proteases and their homologs in the *Drosophila melanogaster* genome: an initial analysis of sequence conservation and phylogenetic relationships. Gene *304*, 117–131.

Ruttkay-Nedecky, B., Nejdl, L., Gumulec, J., Zitka, O., Masarik, M., Eckschlager, T., Stiborova, M., Adam, V., and Kizek, R. (2013). The Role of Metallothionein in Oxidative Stress. Int. J. Mol. Sci. *14*, 6044–6066.

Sedlazeck, F.J., Rescheneder, P., and von Haeseler, A. (2013). NextGenMap: fast and accurate read mapping in highly polymorphic genomes. Bioinformatics *29*, 2790–2791.

Sen, S., and Churchill, G.A. (2001). A statistical framework for quantitative trait mapping. Genetics *159*, 371–387.

Stephan, W., and Li, H. (2007). The recent demographic and adaptive history of *Drosophila melanogaster*. Heredity *98*, 65–68.

Stephan, W., Rodriguez, V.S., Zhou, B., and Parsch, J. (1994). Molecular evolution of the metallothionein gene Mtn in the melanogaster species group: results from Drosophila ananassae. Genetics *138*, 135–143.

Svetec, N., Werzner, A., Wilches, R., Pavlidis, P., Alvarez-Castro, J.M., Broman, K.W., Metzler, D., and Stephan, W. (2011). Identification of X-linked quantitative trait loci affecting cold tolerance in *Drosophila melanogaster* and fine mapping by selective sweep analysis. Mol. Ecol. *20*, 530–544.

Tobari, Y.N. (1993). *Drosophila ananassae*: genetical and biological aspects (Tokyo; Basel; New York: Japan Scientific Societies Press ; Karger).

Vermeulen, C.J., Sørensen, P., Gagalova, K.K., and Loeschcke, V. (2013). Transcriptomic analysis of inbreeding depression in cold-sensitive *Drosophila melanogaster* shows upregulation of the immune response. J. Evol. Biol. *26*, 1890–1902.

Williams, C., Watanabe, M., Guarracino, M., Ferraro, M., Edison, A., Morgan, T., Boroujerdi, A., and Hahn, D. (2014). Cold adaptation shapes the robustness of metabolic networks in *Drosophila melanogaster*. Evol. Int. J. Org. Evol. *68*, 3505–3523.